DOI: 10.24326/fmpmsa.2017.10

CLOTHOID AS A TRANSITION CURVE OF THE MANIPULATOR END-EFFECTOR TRAJECTORY FOR HARVESTING TOMATOES IN A GREENHOUSE

Marek BORYGA, Paweł KOŁODZIEJ, Krzysztof GOŁACKI
University of Life Sciences in Lublin, POLAND
E-mail of corresponding author: marek.boryga@up.lublin.pl

Keywords: precision harvest, trajectory planning, clothoid, tomatoes, greenhouses,

ABSTRACT

The article presents the way of using the clothoid as a transition curve when planning the trajectory of the tomato manipulator end-effector during harvesting in a greenhouse. Three variants of end-effector motion trajectory were planned. The first path consists of two rectilinear segments connected by a circular arc. The second path is composed of a rectilinear segment – clothoid – circular arc – clothoid and a rectilinear segment. The third option consists of two rectilinear segments connected by a biclothoid. For the analysed variants of the manipulator gripper trajectories, the motion parameters were determined and compared, and the results were presented in the graphical form. The algorithm with the use of clothoid, proposed in the paper, ensures the continuity of the displacement, velocity and acceleration for the planned trajectory of the end-effector. This is particularly important for the dynamics of the manipulator arm movement.

INTRODUCTION

The use of robots in greenhouses and orchards, for example for fruit or vegetable harvesting and spraying applications is an important issue for precision agriculture. The first stage of designing technological operations using agricultural manipulators is planning the motion trajectory. The issue concerns two questions: determination of the trajectory of aggregates or mobile robots movement in the area plane as well as that of the end-effector towards a chosen object e. g. a fruit, a vegetable or a stem etc. The paper by Sabelhaus et al. (2013) presents the way of determining the trajectory of recurrent turns whose main construction element is a clothoid. The authors analysed seven different manoeuvres useful from the agronomic point of view and proved that all motions can be executed using the proposed method. Wilde (2009) presented a simple and fast method for calculation of sharpness and curvature of the clothoid for the trajectory of continuous profile. He used the fragments of clothoid to combine rectilinear segments with the circular arc. The algorithm generates smooth, natural, drivable paths using a minimal amount of steering to reach a desired end position. In the case of planning the arm motion, Baur et al. (2013) proposed two approaches to automation determination of the end-effector, trajectory in the working space of the manipulator – heuristic as well as that exploiting an artificial function of the potential. The experimental results are presented and discussed based on harvesting one fruit and one stem. Schuez et al. (2015) proposed a two-stage solution of trajectory planning the redundant manipulator. Motion trajectories are established using the reverse algorithm of kinematics and optimized by the direct method. The paper by Zhang et al. (2016) presents the optimized structure of manipulator with four degrees of freedom. Moreover, the authors stated that the planned cycloidal trajectory of the end-effector motion allows to avoid collision with the obstacle such as a stem, a leaf or other fruit etc. In the paper by Boryga and Graboś (Graboś and Boryga 2013, Boryga 2014) the authors used higher degree polynomials for planning manipulators motion trajectories. Their advantage is the zero value of jerk in the initial and final motion phases which is decisive, any others, for positioning accuracy, dynamic load of driving units and steering the arm motion. In addition, in the paper by Boryga et al. (2015) there was applied the PR-APT (Planning Rectilinear-Arc Polynomial

Trajectory) method for planning the end-effector motion trajectory during harvesting tomatoes in a greenhouse. This paper presents the way of using the clothoid as a transient curve in planning the manipulator end-effector motion trajectory for harvesting tomatoes in a greenhouse. Three variants of end-effector motion trajectory were planned. The first path was composed of two rectilinear segments combined with the circular arc. The second was a rectilinear segment-clothoid-circular arc-clothoid and a rectilinear segment. The third path includes two rectilinear segments combined with the biclothoid (Kobryń 2017). The end-effector motion trajectories defined in this way can constitute partly fragments of obstacle profile to be avoided e. g. tomatoes stem with unripe fruit. For the analysed variants of the manipulator end-effector trajectory the motion parameters courses were determined and compared. Their results are presented graphically.

PLANNING OF MOTION TRAJECTORY

Assumptions

For all trajectories acceleration on the rectilinear segments is described by the 9th degree polynomial (Boryga 2015):

$$a(t) = -p_{252} \cdot t^2 \cdot (t - 0.5t_e)^5 \cdot (t - t_e)^2 \tag{1}$$

where: p_{252} - the polynomial coefficient, t_e - the time of motion end.

On the segment BT_1 the end-effector moves with the positive acceleration (the first part of the polynomial for which $0 \le t < 0.5t_e$), however, for the segment T_2E with negative acceleration (the second part of the polynomial for which $0.5t_e < t \le t_e$).

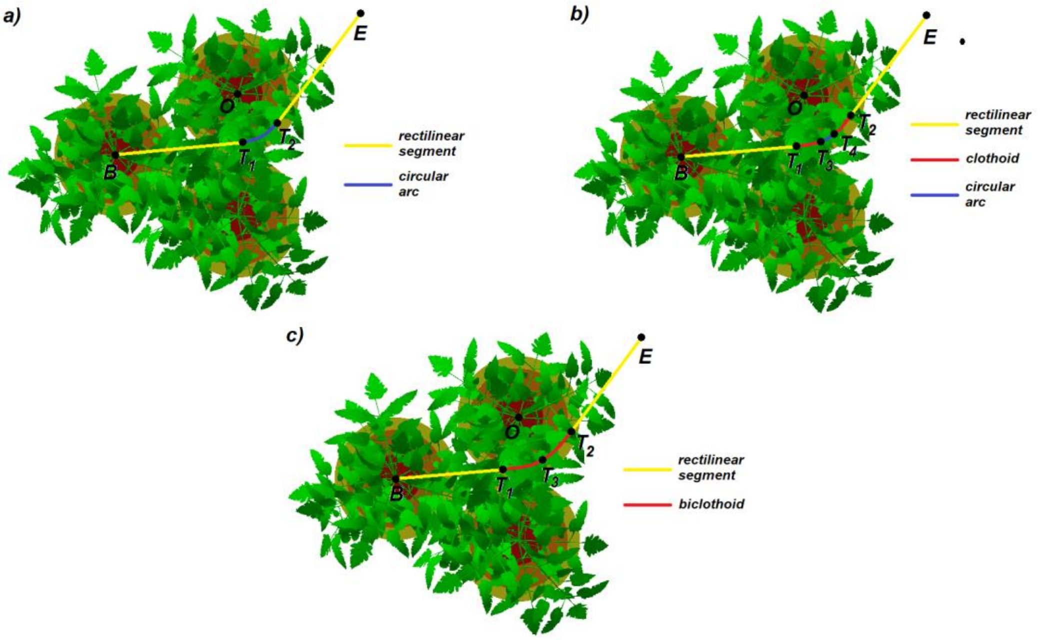

Fig. 1. Planned motion trajectories: a) *Path 1* (rectilinear segment – circular arc – rectilinear segment), b) *Path 2* (rectilinear segment – input clothoid – circular arc – output clothoid – rectilinear segment), c) *Path 3* (rectilinear segment – biclothoid – rectilinear segment)

For all trajectories, the constant variables are:

- The initial point *B* and final point *E* coordinates of the trajectory.
- The arc midpoint *O* and arc radius *R* coordinates constituting a fragment of obstacle outline to be avoided.

- The global coordinates system *xyz* whose origin is in the initial point of trajectory.
- The local coordinates system $x_O y_O z_O$ whose axes are parallel to those of the system *xyz* but the origin is in the point *O*.
- The maximum velocity on the rectilinear segments and the steady velocity of the end-effector on the curvilinear fragments of trajectories - v_{max}.

Calculations for the clothoid segments

The clothoid is a curve whose curvature κ is proportional to the arc length L, expressed by the equations:

$$L = A^2\kappa = \frac{A^2}{R} \quad and \quad \tau = \frac{L^2}{2A^2} = \frac{L}{2R} \tag{2}$$

where: A^2 - the proportionality coefficient (clothoid parameter), τ - arc tangent direction.

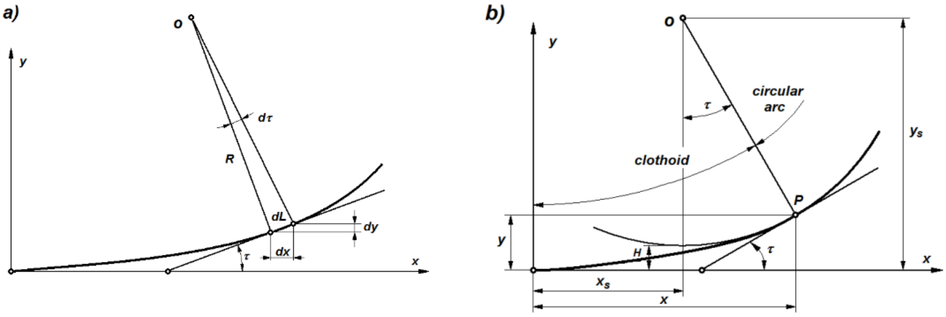

Fig. 2. Construction of an elementary clothoid: a) elementary triangle of clothoid, b) clothoid as a transition curve between rectilinear segments and circular arc

Rectangular coordinates of clothoid (Koc 2015):

$$x = \int_0^L cos\frac{L^2}{2 \cdot A^2} \cdot dL \qquad y = \int_0^L sin\frac{L^2}{2 \cdot A^2} \cdot dL \tag{3}$$

The sequence of steps during calculation procedure of the clothoid segments is as follows:

Step 1. The assumption (*Path 2*) or determination (*Path 3*) of clothoid length as well as calculation of curvature circle distant *H* stand-off from the main tangent, time in the motion along the input and output clothoid and clothoid parameter.

Step 2. Introduction of the coordinate system $x_{T1}y_{T1}z_{T1}$ whose axis x_{T1} is the direction of the motion on the segment BT_1 and its origin is in point T_1 as well as the system $x_{T2}y_{T2}z_{T2}$ whose axis x_{T2} is the direction of the motion on the segment T_2E and the origin is in point T_2.

Step 3. Determination of shifts in time for the motion along the clothoids.

Step 4. Determination of coordinates of the position of the end-effector in motion along: the input clothoid in the system $x_{T1}y_{T1}z_{T1}$, the output clothoid in the system $x_{T2}y_{T2}z_{T2}$, the input and output clothoid in the global coordinate system *xyz*.

Calculation for rectilinear segments

Step 1. Determination of coordinates of tangency points: T_1, T_2 of straight lines crossing points *B* and *E*, respectively as well as tangents to the arc of midpoint in *O* and the radius *R+H* (for the *Path 1 H=0*).

Step 2. Calculation of way increment on the rectilinear segments BT_1 and T_2E denoted Δs^{BT1} and Δs^{T2E}.

Step 3. Determination of motion time on the segments BT_1 and T_2E.

$$t = \frac{\alpha \cdot \Delta s}{\beta \cdot v_{max}} \tag{4}$$

whereby $\alpha = 1/61440$, $\beta = 1/88704$ for the segment BT_1 it is assumed: $\Delta s = \Delta s^{BT1}$, $t = t^{BT1}$ however, for the segment T_2E: $\Delta s = \Delta s^{T2E}$, $t = t^{T2E}$.

Step 4. Determination of polynomial coefficient describing the acceleration course on the BT_1 and T_2E segments:

$$p_{252} = \frac{\beta^{10} \cdot v_{max}^{11}}{\alpha^{11} \cdot (\Delta s)^{10}} \tag{5}$$

For BT_1: $\Delta s = 2 \cdot \Delta s^{BT1}$ and $p_{252} = p_{252}^{BT1}$, for T_2E: $\Delta s = 2 \cdot \Delta s^{T2E}$ and $p_{252} = p_{252}^{T2E}$.

Step 5. Determination of the time shift for the motion on the T_2E segment and coordinates of position of the end-effector in motion along the rectilinear segments.

Calculations for the arc

Step 1. Determination of time of motion along the arc, dependences for calculation of the angle displacement in the local coordinate system $x_O y_O z_O$ and determination of the coordinates of the end-effector position during the motion along the arc in the global coordinate system *xyz*.

Step 2. Determination of time shift for the motion along the arc.

Final calculations

Step 1. Determination of total end-effector dislocation along the trajectory and determination of first and second derivatives of dislocation in relations to time.

Step 2. Determination of total time of motion along the trajectory.

RESULTS OF THE SIMULATION

The path presented in Fig. 3 as a result of simulation refer to the motion in the plane *xy*.

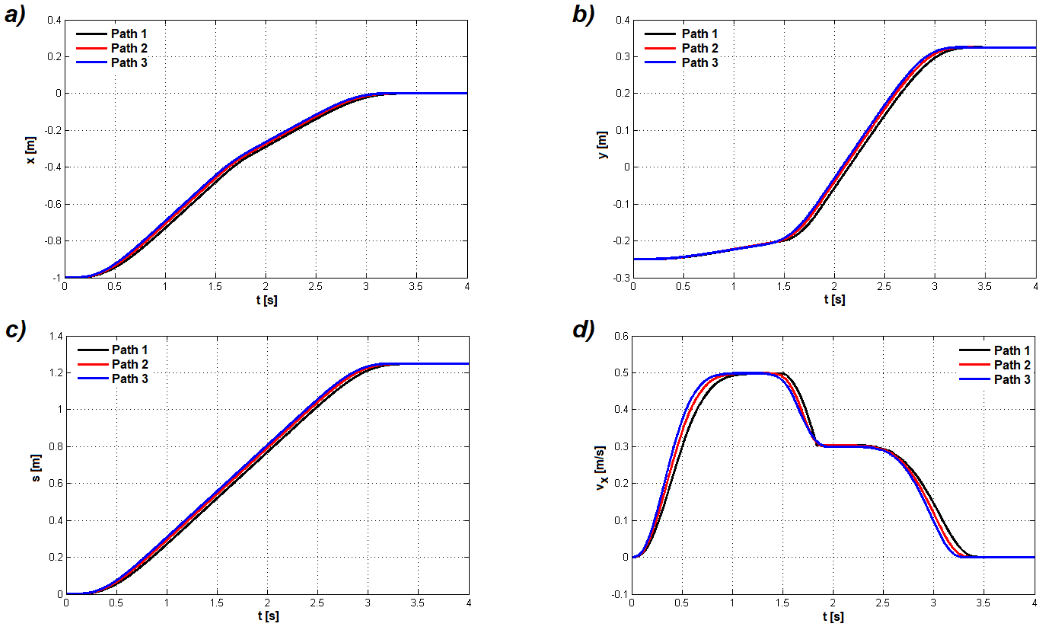

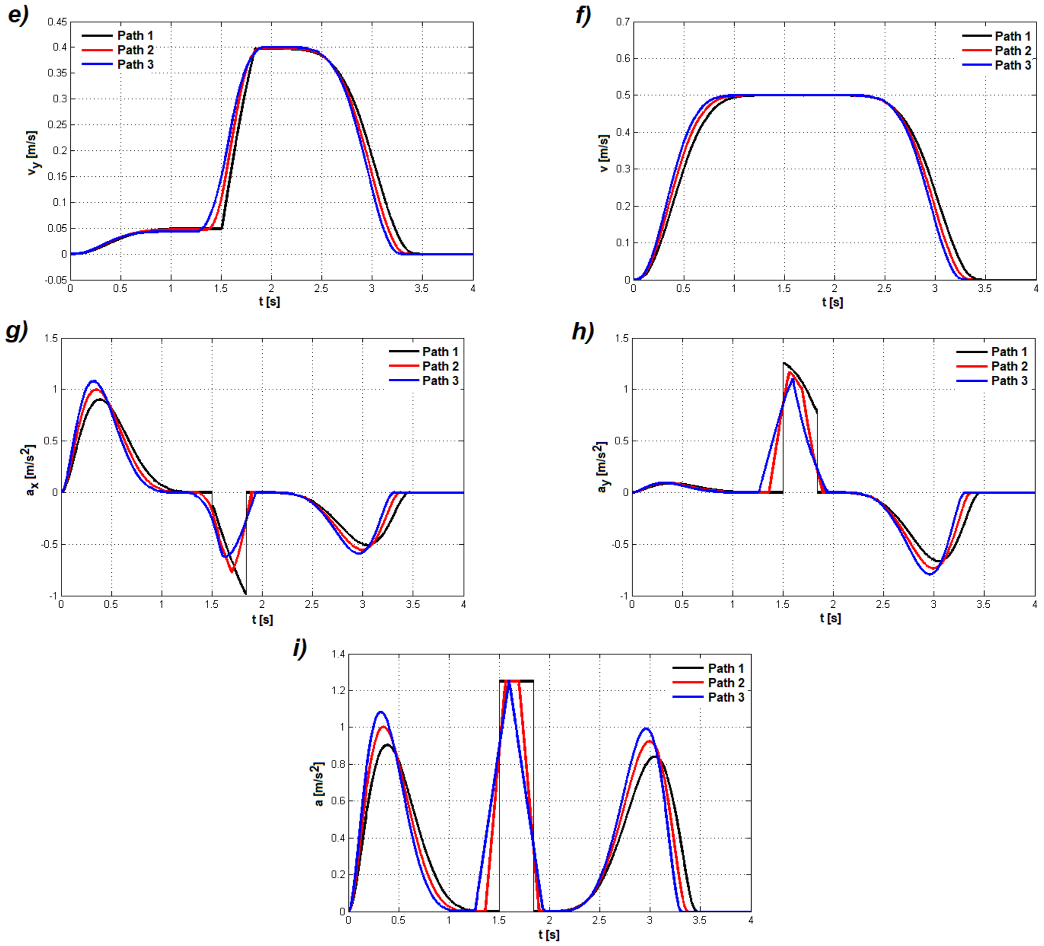

Fig. 3. The courses of kinematic quantities of the end-effector: a) dislocation towards the axis *x*, b) dislocation towards the axis *y*, c) resultant dislocation, d) velocity oriented towards the axis *x*, e) velocity oriented towards the axis *y*, f) resultant velocity, g) acceleration oriented towards the axis *x*, h) acceleration oriented towards the axis *y*, i) resultant acceleration.

Table 1. Comparison of the length of path and time of the motion for individual trajectories

Path denotation	Construction of the path	Length [m]	Motion time [s]
Path 1	Rectilinear segment - BT_1	0.522015	1.507
	Circular arc - T_1T_2	0.164122	0.328
	Rectilinear segment - T_2E	0.561805	1.622
	Σ	**1.247942**	**3.457**
Path 2	Rectilinear segment - BT_1	0.471318	1.361
	Input clothoid - T_1T_3	0.1	0.2
	Circular arc - T_3T_4	0.065660	0.131
	Output clothoid - T_4T_2	0.1	0.2
	Rectilinear segment - T_2E	0.511165	1.476
	Σ	**1.248143**	**3.368**
Path 3	Rectilinear segment - BT_1	0.435984	1.259
	Input clothoid - T_1T_3	0.168475	0.337
	Output clothoid - T_3T_2	0.168475	0.337
	Rectilinear segment - T_2E	0.475936	1.374
	Σ	**1.248870**	**3.307**

The maximal time of motion (3.457s) referred to the shortest *Path 1* of the length 1.2479m. However, the longest equalling 1.2488m with the biclothoid (*Path 3*) was covered in the shortest time which was 3.307s. The character of dislocation courses of the trajectories being analysed for the motion along each axis was similar. Analysing the velocity courses, it was found that for *Path 1* rapid changes of velocity occur in the tangent points T_1 and T_2. In the case of the other trajectories (*Path 2, Path 3*) these changes are also observed out they are of „mild" transitions character. Discontinuities of the course in points T_1 and T_2 are observed only for *Path 1* in the acceleration diagrams. Analysing the motion along the rectilinear trajectory it can be stated, that the maximal absolute acceleration value a_x occurs in point T_2 being 0.989$m \cdot s^{-2}$. Acceleration a_y at point T_1 reaches the maximal value of 1.244$m \cdot s^{-2}$. For *Path 2*, the maximal absolute value a_x is 0.775$m \cdot s^{-2}$ (point T_4). However, the maximal value of the component a_y is 1.178$m \cdot s^{-2}$ (point T_3). For the biclothoid (*Path 3*) the maximal absolute acceleration value a_x is 0.604$m \cdot s^{-2}$ and that of the component a_y is 1.095$m \cdot s^{-2}$

CONCLUSIONS

As follows from the numerical investigations the highest values of components of acceleration in motion along the curvilinear trajectory were found for the trajectory with the circular axis and the lowest for the trajectory with the biclothoid. Translocation, velocity and acceleration for the trajectory, in which the clothoid is use, are continuous functions in the whole range of motion. Moreover, application of polynomial function for description of acceleration causes that its course is tangent towards the time axis in the initial and final points of the trajectory. The above mentioned properties, have a significant effect on increase in positioning accuracy, reduce occurrence of dynamic loads in the manipulator kinematic system, driving energy and time of operation. The algorithm can be implemented in only few steps and therefore, it is very effective.

REFERENCES

Baur, J., Schütz, C., Pfaff, J., Buschmann, T., & Ulbrich, H. (2014). Path Planning for a Fruit Picking Manipulator. *Proceedings International Conference of Agricultural Engineering*, Zurich, 06-10.07.2014.

Boryga, M. (2014). Trajectory planning of an end-effector for path with loop. *Strojniški vestnik - Journal of Mechanical Engineering, 60(12),* 804-814.

Boryga, M., Graboś, A., Kołodziej, P., Gołacki, K., & Stropek, Z. (2015). Trajectory Planning with Obstacles on the Example of Tomato Harvest. *Agriculture and Agricultural Science Procedia, 7,* 27-34.

Graboś, A., & Boryga M. (2013). Trajectory planning of end-effector with intermediate point. *Eksploatacja i Niezawodnosc - Maintenance and Reliability, 15(2),* 182-187.

Kobryń, A. (2017). Use of Polynomial Transition Curves in the Design of Horizontal Arcs. *Roads and Bridges – Drogi i Mosty, 16,* 5-14.

Koc W. (2015). Identification of Transition Curves in Vehicular Roads and Railways. *Logistics and Transport, 4(28),* 31-42.

Sabelhaus, D., Roben, F., Helligen, L.P.M.Z., & Lammers, P.S. (2013). Using continuous-curvature paths to generate feasible headland turn manoeuvres. *Biosystems Engineering, 116(4),* 399-409.

Schuetz, C., Baur, J., Pfaff, J., Buschmann, T., & Ulbrich H. (2015). Evaluation of a Direct Optimization Method for Trajectory Planning of a 9-DOF Redundant Fruit-Picking Manipulator, *Book Series: IEEE International Conference on Robotics and Automation ICRA*, 2660-2666.

Wilde D.K. (2009). Computing Clothoid Segments for Trajectory Generation. *The 2009 IEEE-RSJ International Conference on Intelligent Robots and Systems,* 2440-2445.

Zhang, S.L., Yuan, T., Wang, D.S., Zhang, J.X., & Li, W. (2016). Structure Optimization and Path Planning of Picking Manipulator. *Proceedings of 2016 9th International Symposium on Computational Intelligence and Design ISCID, Vol 2,* 356-360.